Supporting Information

High-Performance Identification of Human Bladder Cancer Using Signal Self-Amplifiable Photoacoustic Nanoprobe

Di Zhang, [†,§] *Ziqi Wang,* [‡,§] *Lu Wang,* [‡] *Zhichao Wang,* [‡] *Hongzhi Wang,* [‡] *Guangbin Li,* [‡] *Zeng-Ying Qiao,* [†,*] *Wanhai Xu,* [‡,*] *and Hao Wang*[†,*]

[†]CAS Center for Excellence in Nanoscience, CAS Key Laboratory for Biomedical Effects of Nanomaterials and Nanosafety, National Center for Nanoscience and Technology (NCNST), Beijing, 100190, China

[‡]Department of Urology, the Fourth Hospital of Harbin Medical University, Heilongjiang Key Laboratory of Scientific Research in Urology, Harbin, 150001, China.

KEYWORDS: Self-assembly, Photoacoustic, Nanoprobe, Cancer, Bioimaging

Materials. Penicillin and streptomycin, Phosphate-Buffered Saline (PBS), Fetal Bovine Serum (FBS), DMEM (Dulbecco's Modified Eagle Medium) medium and Trypsin were obtained from HyClone/Thermofisher (Beijing, China). Squaraine (SQ) was synthesized as described previously.[1] 96-well culture plates were purchased from Coning Company. CCK-8 (Cell counting kit-8) was purchased from Beyotime Institute of Biothechnology (Shanghai, China). All the other solvents used in the research were purchased from Sinopharm Chemical Reagent Beijing Co., Ltd or Beijing Chemical Company (China).

Properties of P18 in Different Polarity Solution. UV/Vis absorption, fluorescent and photoacoustic (PA) signal intensity changes of P18 were investigated by the same protocol of our previous reported.[2] Briefly, P18 was dissolved in dimethyl sulfoxide (DMSO) with the concentration of 1 mM. In UV/Vis (mode: UV-2600, wavelength range: 500 nm-800 nm, slit width: 1.0, measurement mode: absorption) absorption study, the concentration of P18 was diluted to 10 μM with different ratio of DMSO and PBS (0-99% of water). The fluorescent intensity of P18 at the same ratio of DMSO and PBS was measured with the excitation wavelength at 700 nm, and the emission wavelength at 720 nm with fluorescence spectrometer (mode: F-280). The PA signal intensity was also carried out with these solutions. The solution with different ratio of water and DMSO was injected into the agarose patterns and scanned utilized the multispectral optoacoustic tomography (MSOT 128, 750 nm).

Investigation of Photothermal Conversion of P18. The solutions of P18 (500 μL) in H_2O and DMSO were injected into polydimethylsiloxane (PDMS) chambers, respectively. The temperatures of respective solutions were recorded through thermal camera under the laser irradiation at wavelength of 750 nm (150 mW/cm^{-2}).

Calculate the enhanced PA signal. The photothermal conversion efficiency of P18 monmers in DMSO and aggregates in H_2O was calculated according the reported literature.[3]

To investigate the PA signal, the value of η should be calculated firstly and the related equations as follow:

The equation of absorption coefficient (μ_a, cm^{-1}) as follow:

$$\mu_a = \sigma M N_A \quad (1)$$

$$\sigma = 1000 \ln (10) \varepsilon / N_A \quad (2)$$

Where σ was absorption cross section, ε was molar absorption coefficient, N_A was Avogadro's number.

Γ was Grueneisen parameter (dimensionless), equation as follow：

$$\Gamma = c^2 \beta / C_p \quad (3)$$

Where c was the speed of acoustic monitored in MOST, β was the volume expansion coefficient, C_p was the isobaric heat capacity (4.2 J / mol•K).

$$\eta = \beta / C_p = [hs (T_{max} - T_{evir.}) - Q_{dis}] / I (1-10^{-Ab700}) \quad (4)$$

$$hs = m C_p / r_s \quad (5)$$

$$r_s = -Ln (\theta) / t \quad (6)$$

$$\theta = (T - T_{evir}) / (T_{max} - T_{evir.}) \quad (7)$$

Where T_{max} was the maximum temperature increase of the solution under irradiation time (1 min), T_{evir} was the temperature of the environment, Ab_{700} was the absorption of the **P18** at 700 nm, m was the mass of the solution of the **P18** dissolved, t was the irradiation time, I was the power of the laser (150 mW/cm^{-2}), and r_s was the slope of the line of time dependent -Ln (θ). Q_{dis} was ignored due to the same value with different solution.

Circular Dichroism (CD) Spectra. The spectra were obtained using a CD spectrometer (JASCO J 1500, Japan) with a cell path length of 1 mm at room temperature. The measurements were performed at a scanning speed of 500 nm min^{-1} and a resolution of 0.5 nm. The spectra were corrected by subtracting the solution background. For each sample, three spectras were obtained and averaged. Results for CD spectra are expressed in terms of molar ellipticity.

Cytotoxicity of P18/AHC⊂L. MCF-7 cells were cultured in DMEM supplemented with 10% FBS at 37 °C in a humified atmosphere containing 5% CO_2. And then the cells were seeded in 96-well plates at a density of 1×10^5 cells per well. After 15 h adhesion, **AHC⊂L**, **P18⊂L** and **P18/AHC⊂L** with different concentrations (caculation from P18, 1-20 μM) were added into the medium and cultured for 24 h at 37 °C in a humified atmosphere containing 5% CO_2. And then the cell viability of different treatments was investigated by the cell counting kit-8 assay (CCK-8) after 1 min lasr irradiation (750 nm, 150 mW). For CCK-8 assay, the supernatant was removed and washed with PBS twice, and then 200-μL fresh culture medium supplemented with 10% FBS and 1% penicillin and streptomycin was added into the wells. Subsequently, the solution of CCK-8 (20 μL) was added to the wells followed by 4 h incubation at 37 ^oC in a humified atmosphere containing 5% CO_2. Finally, the absorbance values of the cells per well were determined with a Microplate reader at 419 nm for analyzing the cell viability. Control experiments were done with addition the same volume of PBS and the other treatments were under the same condition. The cell viability rate was calculated through the equation as follow:

$$\text{The cell viability} = A_s/ A_c\times 100\%$$

Where the A_s was the absorbance of the treatments of **P18/AHC⊂L** or **P18⊂L** with different concentrations, A_c was the absorbance of the control treatments with PBS.

***In Vivo* PA Imaging Study.** All animals were treated in accordance with the Guide for Care and Use of Laboratory Animals, approved by the Committee for Animal Research of National Center for Nanoscience and Technology, China. MCF-7 cells (5×10^6) in PBS (100 μL) solution were subcutaneously injected into the right flank of a BALB/c nude mice. The initial body weight of mice was about 17-18 g. After two weeks of tumor formation, **P18/AHC⊂L** (100 μM, 200 μL) dispersed into PBS was intravenous injected into mice

through tail vein. After the injection, the mice were scanned with MSOT (mode: MSOT 128, excitation wavelength at 750 ±1 nm) at different time intervals (0.5 h, 1 h, 2 h, 4 h and 6 h).

***In Vivo* Distribution of CD44v6-Probe.** EJ human bladder cells (5×10^6) in PBS (100 μL) solution were subcutaneously injected into the right flank of a BALB/c nude mice. The initial body weight of mice was about 17-18 g. After two weeks of tumor formation, SQ, a near-infrared (NIR) fluorescent dye, labeled CD44v6-P18⊂L and CD44v6-P18/AHC⊂L **P18/AHC⊂L** (100 μM, 200 μL) dispersed into PBS was intravenous injected into mice through tail vein, respectively. After 4 h, the mice were anaesthetized, placed in the chamber of an *in vivo* imaging system, and whole body images were acquired. Mice treated with intravascular injection PBS were acted as control group. Then animals were killed and tumor, heart, liver, spleen, lung and kidney were excised for flourecsent intensity measurement. All images were analyzed and collected with a PerkinElmer (Spectrum CT) *in vivo* imaging system (excitation filter, 680 nm; emission filter, 700 nm).

Tissue Samples. With the approval of the local institutional review board, total 12 samples of normal urothelial and cancer tissue were obtained from the patients with bladder biopsy, transurethral resection or radical cystectomy at the Department of Urology, the 4th hospital of Harbin Medical University, Harbin, Heilongjiang Province, China. Paraffin-embedded specimens were processed by routine histological techniques. Microscope slides were stained with haematoxylin and eosin (H&E) and evaluated under an optical microscope by an experienced pathologist in the same hospital, who reviewed all the original H&E-stained slides, given the diagnoses, and classified the tumour stage and grade according to the protocol.[4]

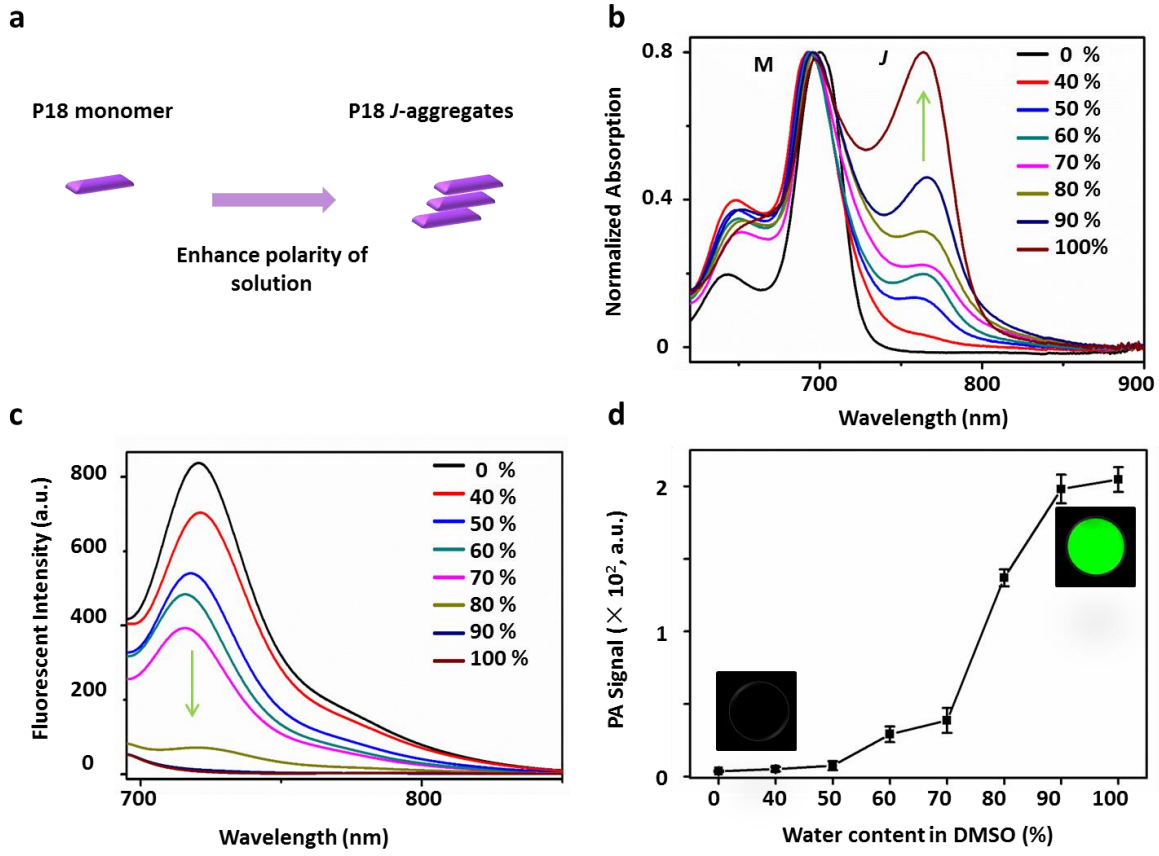

Figure S1. a) Schematic illustration of P18-aggregates formation after enhancing the polarity of solution. UV/Vis absorption b), fluorescent signal intensity changes c) and photoacoustic signal intensity d) of P18 with changing the polarity of solution (water content in DMSO: 0-100%, v/v). The values were expressed as mean ± SD (N = 3).

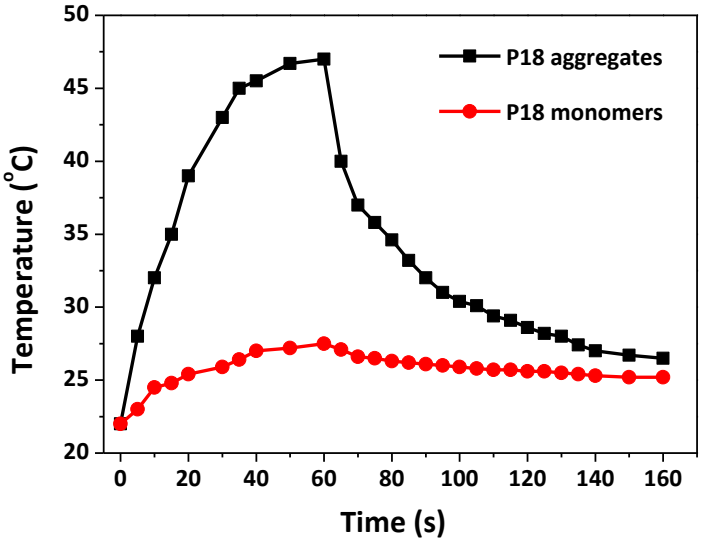

Figure S2. Heating/cooling curves of P18 aggregates (in H_2O) and monomers (in DMSO). The energy input from lasers was 150 mW at 750 nm with an irradiated diameter of 4 mm.

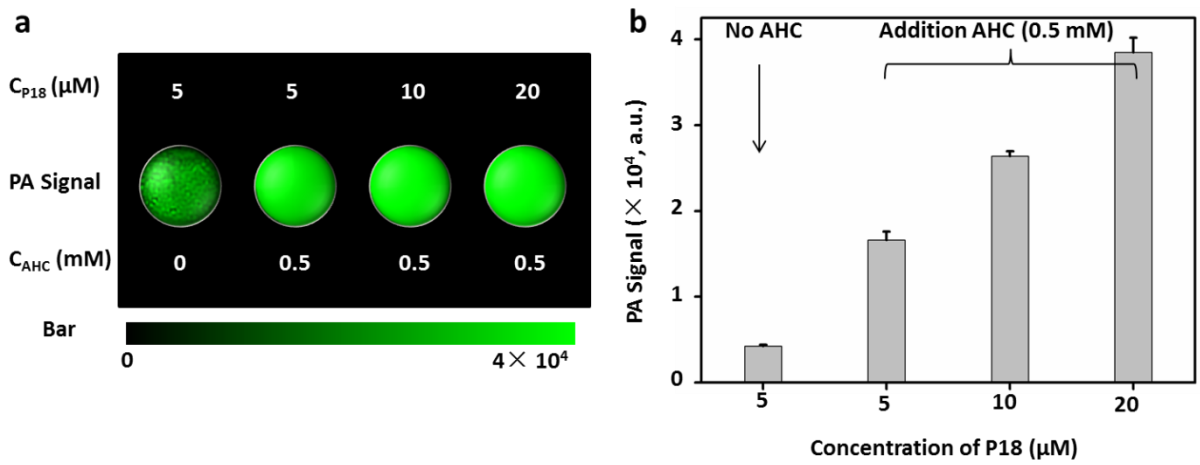

Figure S3. PA images a) and the quantification b) of the photoacoustic signal intensity amplification of **P18/AHC⊂L** with different P18 concentrations. The values were expressed as mean ± SD (N = 3).

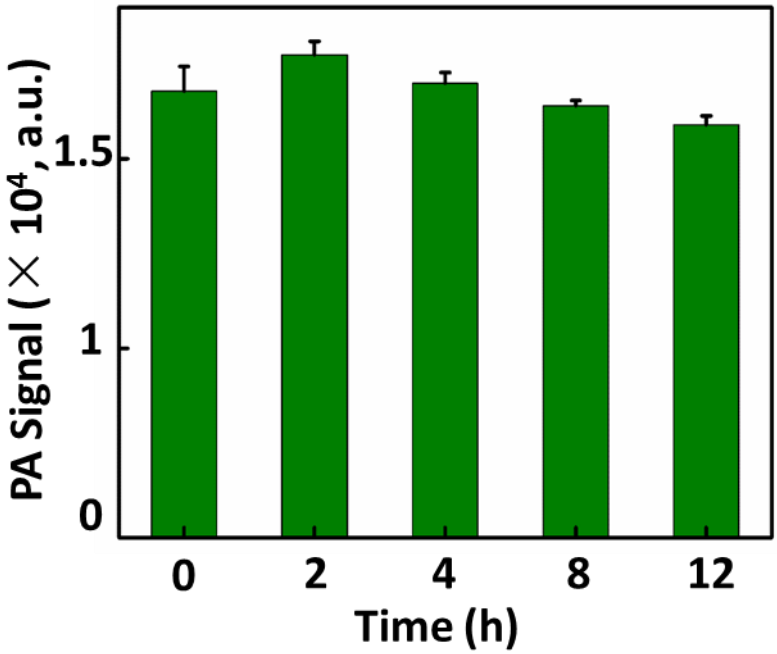

Figure S4. PA signal changes of **P18/AHC⊂L** at different time points in 12 h under interval laser irradiation every 2 h. P18 concentration: 10 μM. The values were expressed as mean ± SD (N = 3).

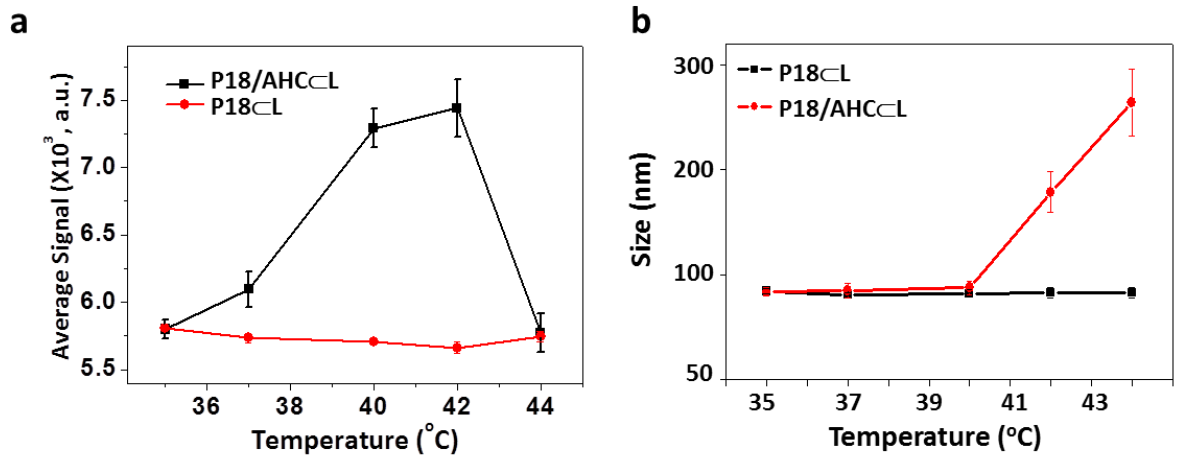

Figure S5. Photoacoustic signal intensity a) and hydrodynamic diameter b) of **P18/AHC⊂L** and **P18 ⊂L** solutions at various temperatures. The solutions were kept at each temperature for 2 min. P18 concentration: 10 μM. The values were expressed as mean ± SD (N = 3).

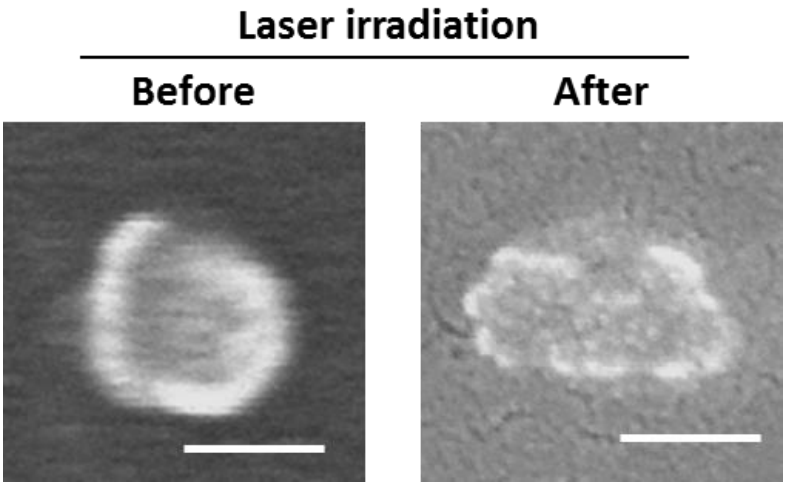

Figure S6. The morphology change of **P18/AHC⊂L** nanoprobe before and after laser irradiation observed by SEM images. P18 concentration: 10 μM; AHC concentration: 0.5 mM. Titanium-doped sapphire femtosecond pulse laser, 750 nm, 150 mW. Scale bars, 80 nm.

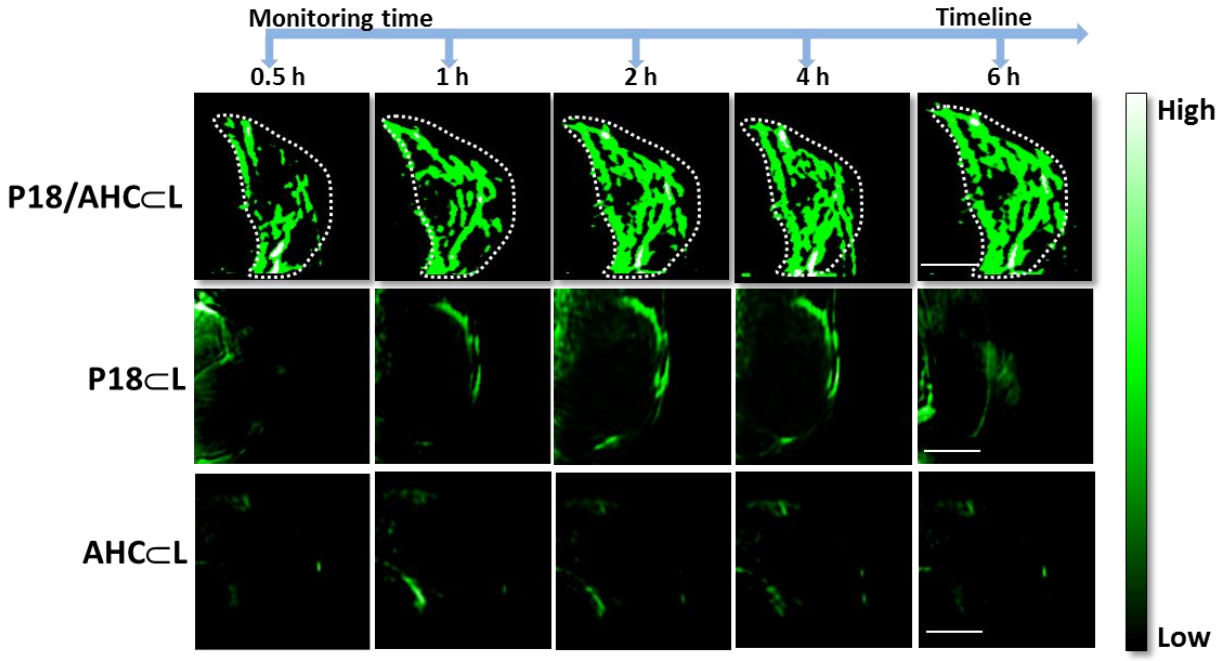

Figure S7. PA imaging of tumor in MCF-7 xenografted mice after treated by **AHC⊂L**, **P18⊂L** and **P18/AHC⊂L** for 6 h. The white dashed circles indicate the outlines of tumor site of mice. Scale bars, 2 mm.

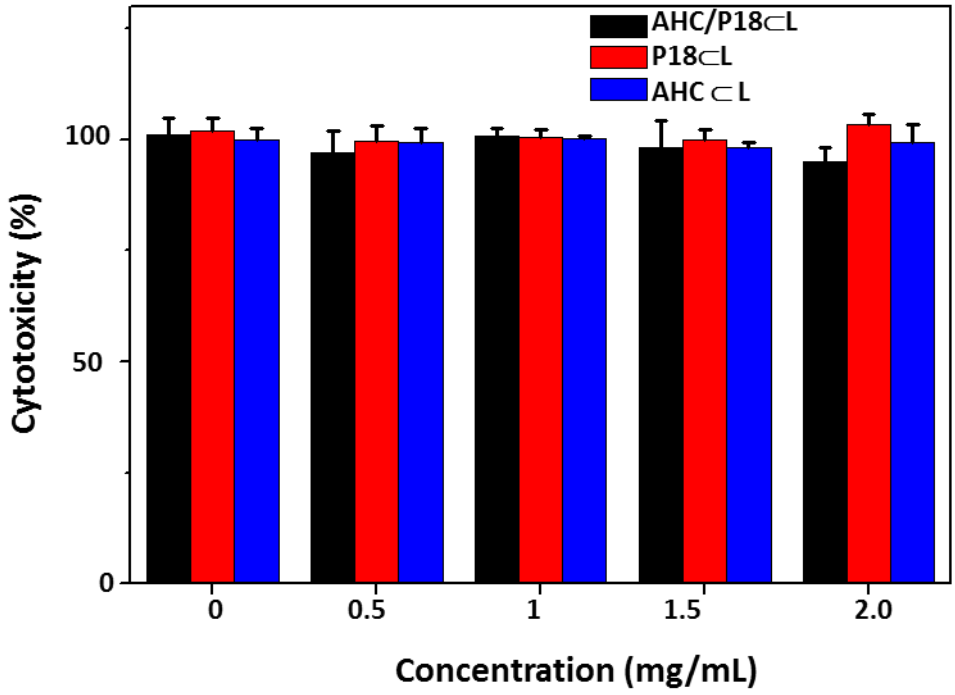

Figure S8. Cell viability assay of MCF-7 cell lines treated with a series of concentrations of **AHC⊂L**, **P18⊂L** and **P18/AHC⊂L** after 1 min laser irradiation (750 nm, 150 mW). Data were expressed as mean ± SD (n = 4) and the experiment were repeated twice.

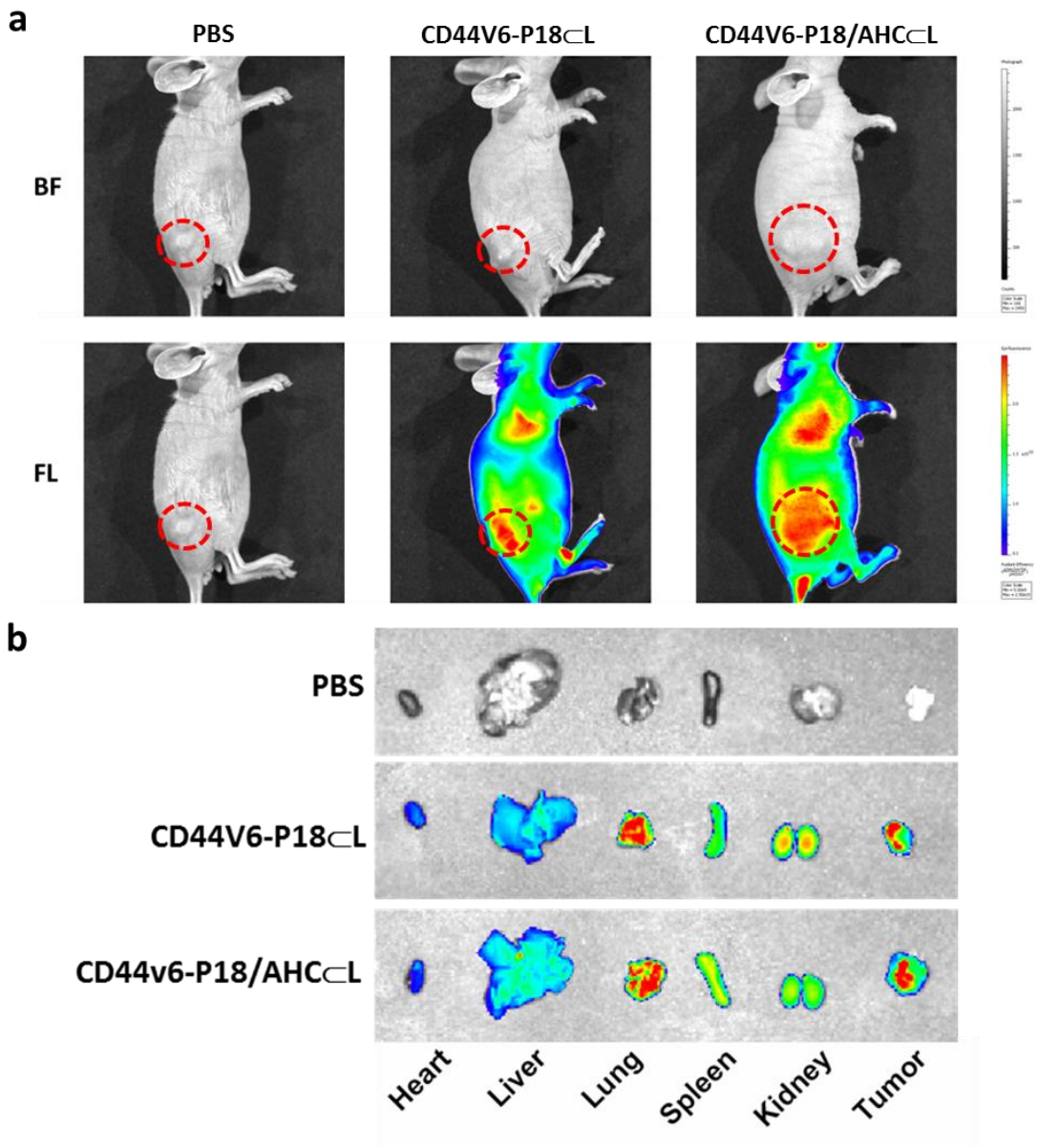

Figure S9. a) *In vivo* NIR imaging of nude mice bearing U87 tumors after tail-vein injection of PBS, **CD44v6-P18⊂L** and **CD44v6-P18/AHC⊂L** at 4 h. The red dashed circles indicate the outlines of tumor site of mice. b) *Ex vivo* NIR imaging of tissues and tumors at 4 h after the intravenous administration of PBS, **CD44v6-P18⊂L** and **CD44v6-P18/AHC⊂L**. c) Quantitative analysis for the biodistribution of nanoprobes in major organs. Values were expressed as means ± SD (N = 3).

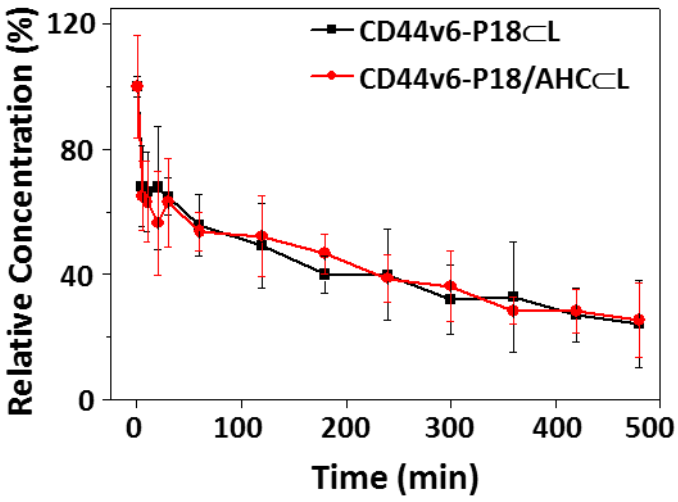

Figure S10. Plasma nanotherapeutics concentration in mice following tail-vein injection of **CD44v6-P18⊂L** and **CD44v6-P18/AHC⊂L**. Values were expressed as means ± SD (N = 3).

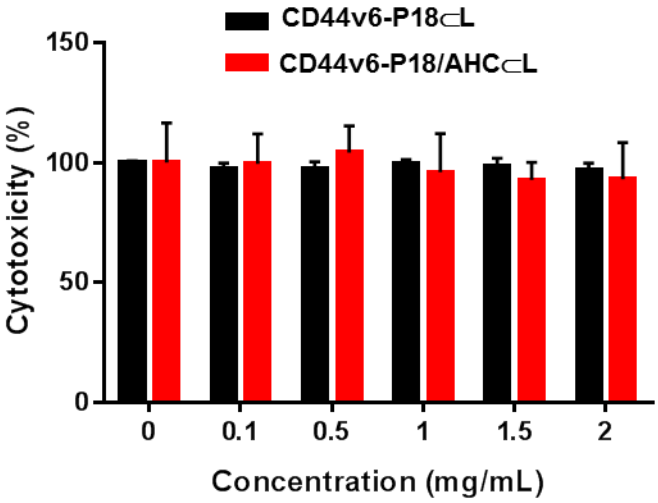

Figure S11. Cell viability assay of EJ cell lines treated with a series of concentrations of **CD44v6-P18⊂L** and **CD44v6-P18/AHC⊂L** after 1 min lasr irradiation (750 nm, 150 mW). Data were expressed as mean ± SD (n = 4) and the experiment were repeated twice.

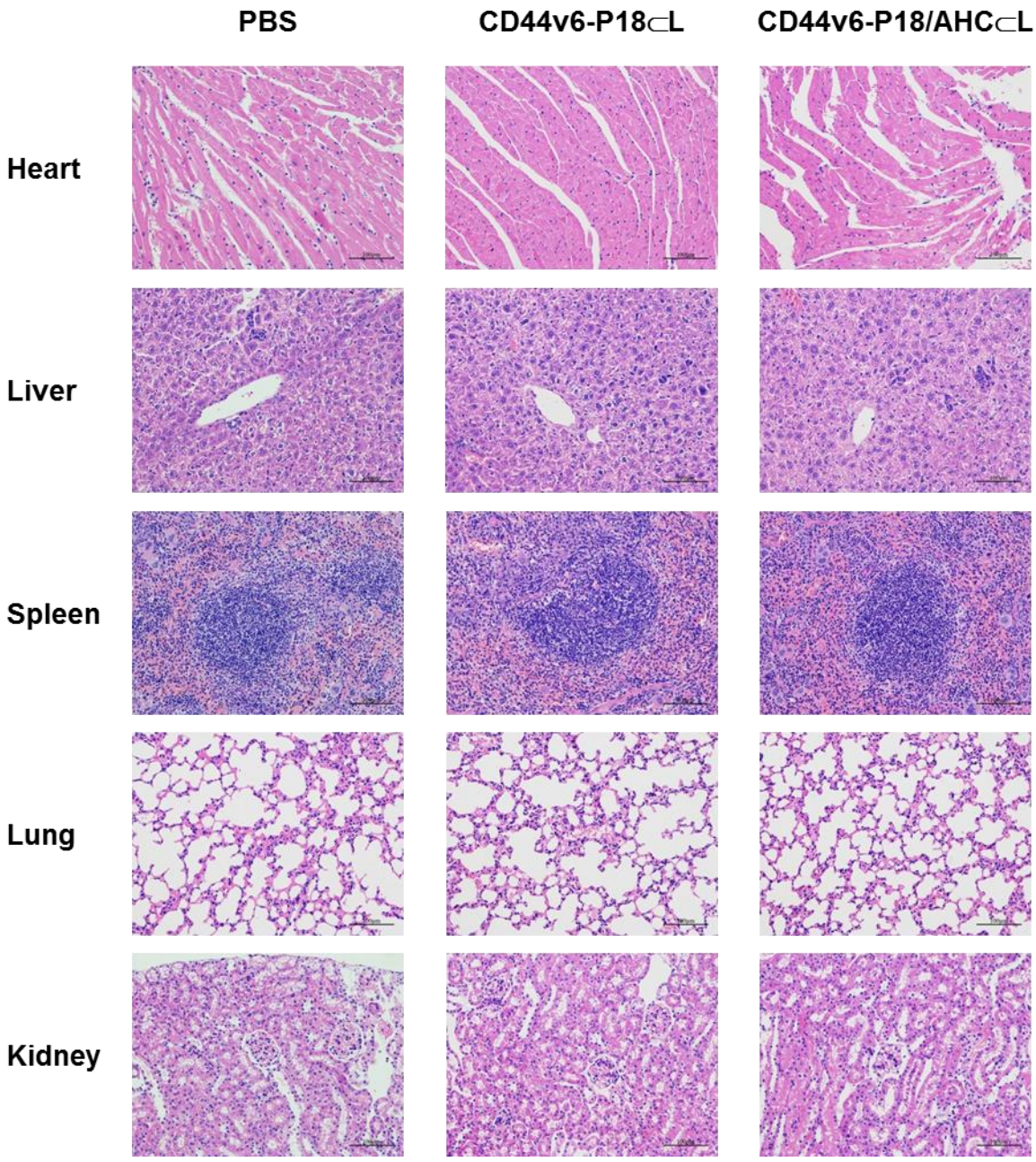

Figure S12. Representative photomicrographs of the heart, liver, spleen, lung and kidney sections (H&E staining) of mice treated with **CD44v6-P18⊂L** and **CD44v6-P18/AHC⊂L**.

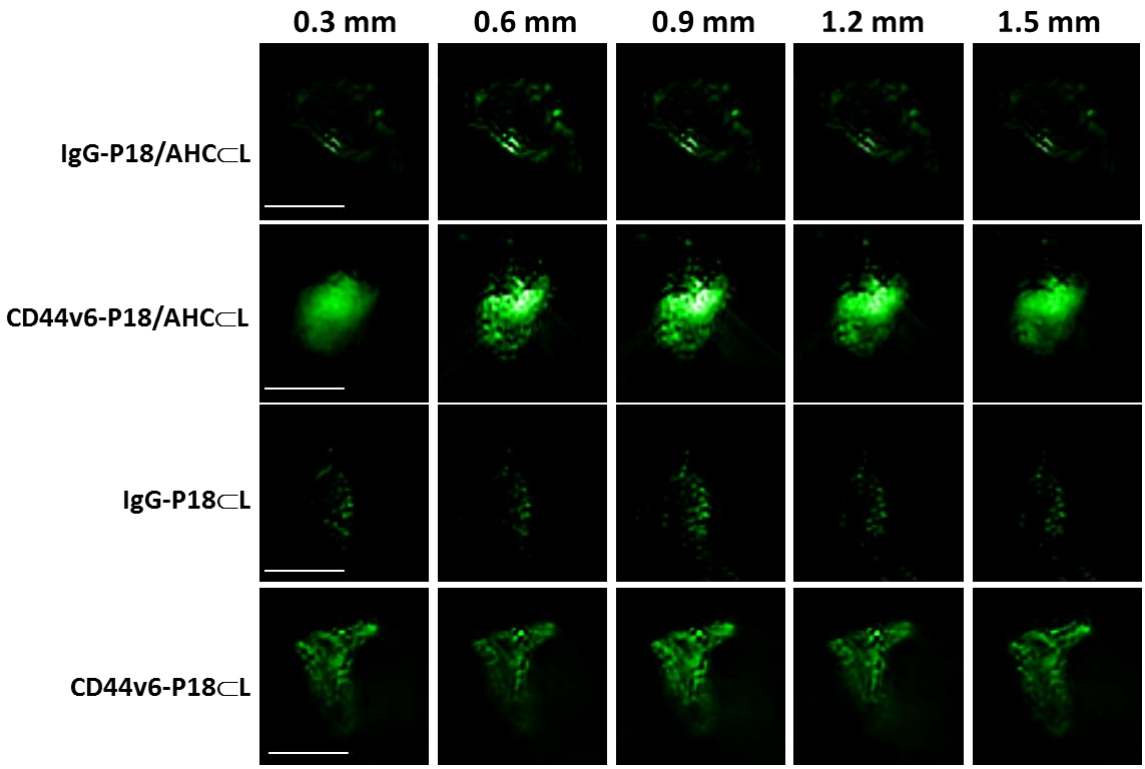

Figure S13. The PA imaging of tumor tissue after treatment with IgG-probe and CD44v6-probe at different depths from 0.3 mm to 1.5 mm. Scale bars, 3 mm.

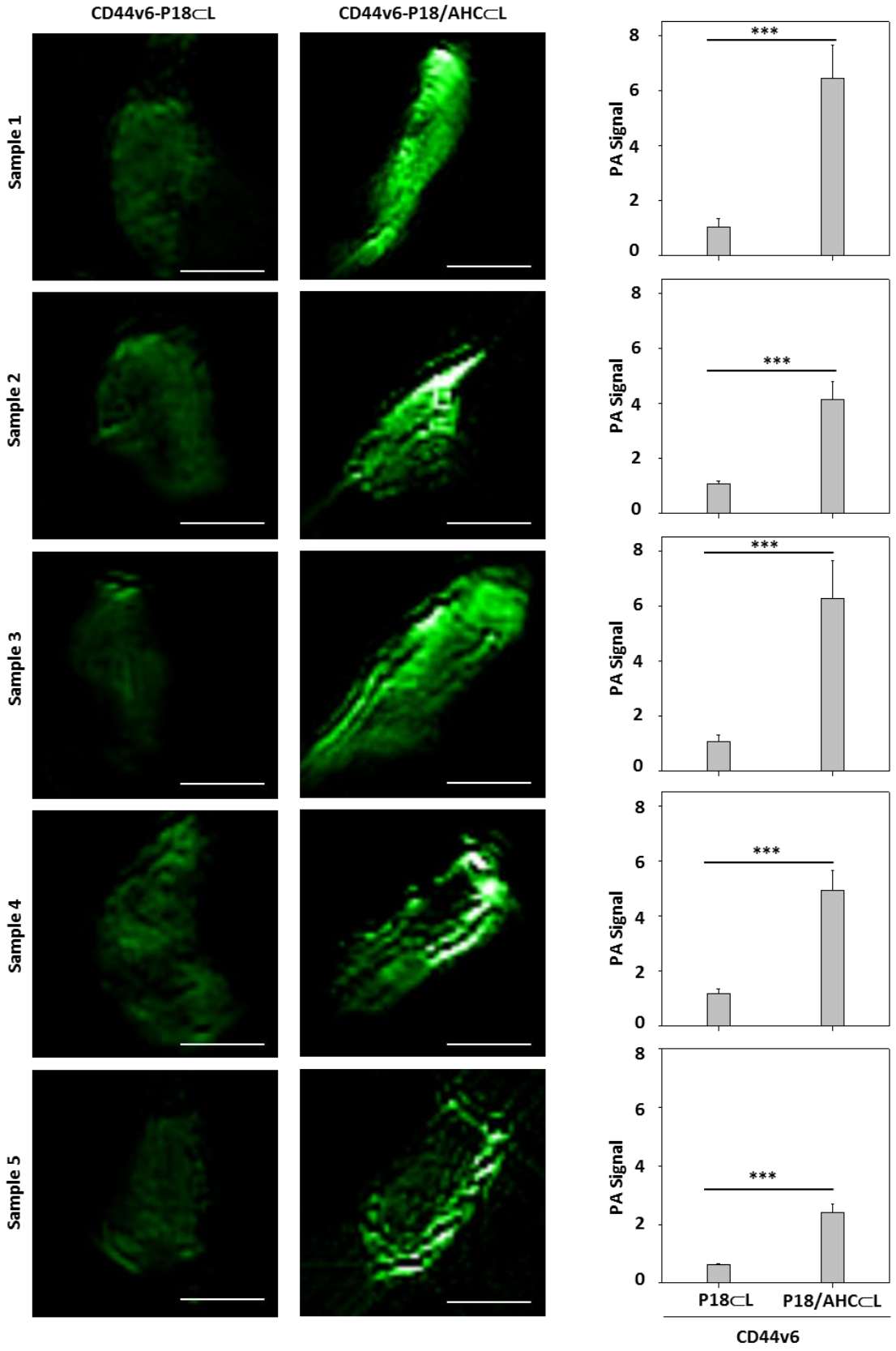

Figure S14. The PA imaging of tumor tissue after treatment with CD44v6-probe (Left) and corresponding expression scores in each group (Right). The values were expressed as mean ± SD (N = 5). Asterisks (*) denote the statistical significance: ***$p < 0.001$. Scale bars, 2 mm.

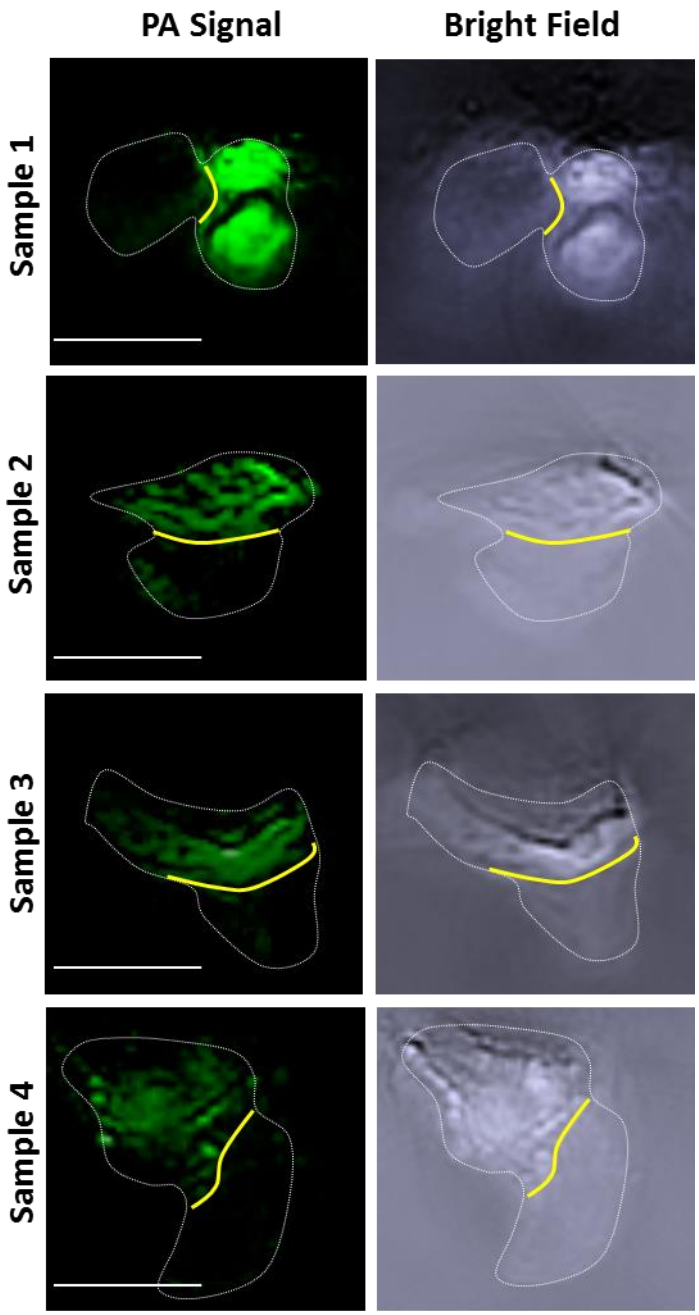

Figure S15. The PA imaging of tumor boundary (include normal and tumor tissue) that treated with **CD44v6-P18/AHC⊂L**. Scale bars, 3 mm.

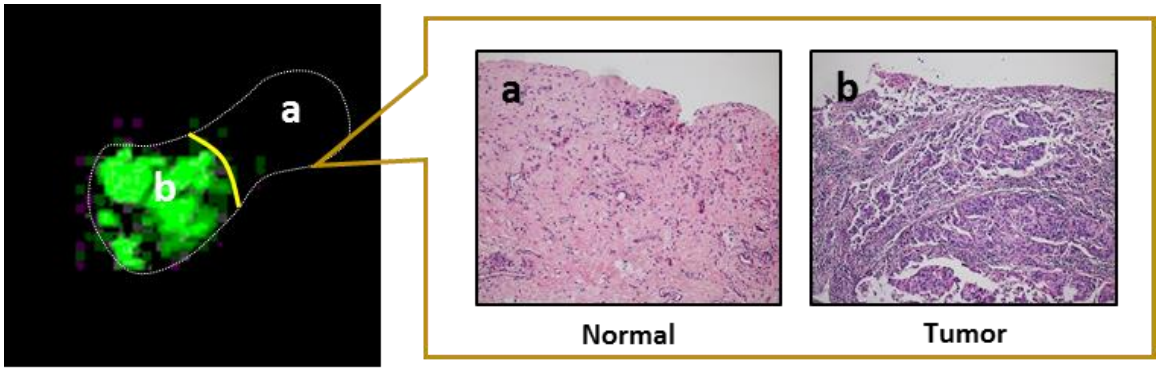

Figure S16. The PA imaging of normal and tumor tissue and corresponding H&E images.

Reference

(1) Mayerhoeffer, U.; Deing, K.; Gruss, K.; Braunschweig, H.; Meerholz, K.; Würthner, F., Outstanding Short-Circuit Currents in BHJ Solar Cells Based on NIR-Absorbing Acceptor-Substituted Squaraines. *Angew. Chem. Int. Ed.* **2009,** *48*, 8776-8779.

(2) Zhang, D.; Qi, G.-B.; Zhao, Y.-X.; Qiao, S.-L.; Yang, C.; Wang, H., In Situ Formation of Nanofibers from Purpurin18-Peptide Conjugates and the Assembly Induced Retention Effect in Tumor Sites. *Adv. Mater.* **2015,** *27*, 6125-6130.

(3) Liu, W.-J.; Zhang, D.; Li, L.-L.; Qiao, Z.-Y.; Zhang, J.-C.; Zhao, Y.-X.; Qi, G.-B.; Wan, D.; Pan, J.; Wang, H., In Situ Construction and Characterization of Chlorin-Based Supramolecular Aggregates in Tumor Cells. *ACS Appl. Mater. Interfaces* **2016,** *8*, 22875-22883.

(4) L. H. Sobin, Ch. Wittekind, TNM classification of malignant tumours (6th edition). New York: Wiley-Liss, Inc., **2002**.